Int. J. Oral Maxillofac. Surg. 2019; 48: 810–823
https://doi.org/10.1016/j.ijom.2018.09.003, available online at https://www.sciencedirect.com

International Journal of Oral & Maxillofacial Surgery

Randomised Clinical Trial
Pre-Implant Surgery

A randomized clinical trial evaluating maxillary sinus augmentation with different particle sizes of demineralized bovine bone mineral: histological and immunohistochemical analysis

R. S. de Molon[1], F. S. Magalhaes-Tunes[2], C. V. Semedo[2], R. G. Furlan[2], L. G. L. de Souza[2], A. P. de Souza Faloni[2], E. Marcantonio Jr[1], R. S. Faeda[2]

[1]Department of Diagnosis and Surgery, School of Dentistry at Araraquara, São Paulo State University – UNESP, Araraquara, São Paulo, Brazil; [2]Department of Health Sciences, Implantology Post Graduation Course, University Centre of Araraquara – UNIARA, São Paulo, Brazil

R. S. de Molon, F. S. Magalhaes-Tunes, C. V. Semedo, R. G. Furlan, L. G. L. de Souza, A. P. de Souza Faloni, E. Marcantonio Jr, R. S. Faeda: A randomized clinical trial evaluating maxillary sinus augmentation with different particle sizes of demineralized bovine bone mineral: histological and immunohistochemical analysis. Int. J. Oral Maxillofac. Surg. 2019; 48: 810–823.

Abstract. This study was performed to investigate sinus floor augmentation with two different particle sizes of demineralized bovine bone mineral (DBBM) by means of histological and immunohistochemical (IHC) analysis. A randomized clinical trial was conducted involving 10 individuals requiring two-stage bilateral maxillary sinus augmentation for implant installation. The patients were randomly divided into two groups following a split-mouth design: the maxillary sinus on one side was filled with small-sized particles (0.25–1 mm) and on the contralateral side with large-sized particles (1–2 mm). After a healing period of 8 months, 25 implants were placed. During implant site preparation, bone biopsies were obtained from each sinus, perpendicular to the long axis of the implant (buccal–palatal direction), for descriptive and histomorphometric analyses. IHC staining for protein expression of osteocalcin (OCN), vascular endothelial growth factor (VEGF), and tartrate-resistant acid phosphatase (TRAP) was also performed. Histomorphometric analysis revealed no statistically significant difference in the percentage of biomaterial (32.4 ± 8.56% and 38.0 ± 6.92%), newly formed bone (36.1 ± 9.60% and 36.7 ± 5.79%), or connective tissue (30.4 ± 8.63% and 23.8 ± 6.16%)

0901-5027/060810 + 014

between the small- and large-sized particle groups, respectively. IHC analysis did not reveal differences in the expression of OCN, VEGF, or TRAP. These findings suggest that both particle sizes of DBBM are effective for bone augmentation in the maxillary sinus.

Key words: Bio-Oss; bone graft; dental implants; maxillary sinus; sinus floor augmentation.

Accepted for publication 10 September 2018
Available online 13 November 2018

Maxillary sinus floor augmentation, a surgical technique that allows the installation of implants of proper length[1], is accomplished by lifting the sinus membrane and placing biomaterials or autogenous/exogenous bone grafts, thereby providing long-term implant stability[2]. Demineralized bovine bone mineral (DBBM) (Bio-Oss; Geistlich Pharma AG, Wolhusen, Switzerland) is an osteoconductive material, with crystallinity and physical and morphological properties similar to those of human cancellous bone. It provides a scaffold and a matrix for osteogenic cell migration from the sinus wall to the graft particles, increasing the potential for new bone formation[3,4]. Several clinical studies have demonstrated high long-term success rates, predictability, and longevity when DBBM is used for bone augmentation procedures[2,5–9]. With its micro- and macro-pores, Bio-Oss presents hydrophilic characteristics, and this feature plays an important role in bone revascularization and neoformation in the maxillary sinus[10]. Moreover, DBBM has several advantages compared to autogenous bone, such as unlimited quantity available, biocompatibility, osteoconductive proprieties[11], low resorption rate, minimal risk of immunological rejection, and lower morbidity for the patient.

This research group recently performed a randomized clinical trial to evaluate the stability of dental implants installed in the posterior region of the maxilla after sinus floor augmentation with two different particle sizes of Bio-Oss[7]. It was found that both particle sizes of DBBM resulted in good implant stability, confirmed by the increased torque values for implant insertion and high implant stability quotient measured by means of resonance frequency analysis. There were no differences between the two particle sizes in any of the measurements performed.

Testori et al.[9] evaluated bone formation and residual graft volume at 6–8 months after bilateral sinus augmentation grafted with large (1–2 mm) or small (0.25–1 mm) particle sizes of DBBM by means of histological and histomorphometric analysis. The results indicated that the large-sized particles presented significantly more bone formation (26.77 ± 9.63%) than the small-sized particles (18.77 ± 4.74%), reaffirming its possible use for sinus augmentation. Furthermore, osteocytes and osteoblasts were present in the newly formed bone for both particle sizes. Similarly, Chackartchi et al.[8] evaluated the newly formed bone, histologically and radiographically, in maxillary sinuses grafted with different particle sizes of DBBM. They showed that the two granule sizes led to the same pattern of bone formation, with no differences in the amount of newly formed bone between the groups. Descriptive histology also showed multinucleated giant cells in intimate contact with the small sized-particles more than with the large-sized particles. They concluded that both particle sizes were effective for maxillary sinus augmentation.

While Bio-Oss, the most widely used DBBM graft biomaterial, has frequently been used as a bone graft alternative, with several clinical studies reporting active bone neoformation and high success rates after maxillary sinus augmentation[2,5,7–9,12–14], only a small number of studies in the literature have investigated the effect of different particle sizes of DBBM on protein expression after sinus lift. Thus, the aim of this randomized controlled clinical trial was to compare the effects of different particle sizes of DBBM for maxillary sinus floor augmentation by means of descriptive and histomorphometric analyses and immunohistochemical (IHC) examinations for protein expression of vascular endothelial growth factor (VEGF), osteocalcin (OCN), and tartrate-resistant acid phosphatase (TRAP) 8 months after the sinus lifting procedure.

Materials and methods

This randomized clinical study followed all guidelines of the Consolidated Standards of Reporting Trials (CONSORT) statement[15]. The study procedure was approved by the Ethics Committee on Human Research before patient enrolment. All subjects involved were fully informed about the study protocol and a written informed consent form was obtained from all patients prior to the initial treatment.

Patients and study design

The study design was based on that used in a previous study[7]. Briefly, patients were recruited at the Implantology Department of Araraquara School of Dentistry – UNIARA from March 2015 through November 2015. A total of 10 patients were registered in this clinical trial; six patients were female and four were male, and they ranged in age from 30 to 65 years (mean age 48.34 ± 12.83 years). Eight patients were partially edentulous and two patients were totally edentulous. Demographic and clinical data for all of the study patients are given in Table 1.

The inclusion criteria were as follows: patients who required bilateral sinus floor augmentation for implant installation (two-stage surgery) in the posterior maxillary region with residual bone height of <5 mm (based on panoramic radiographs). The exclusion criteria were: compromised general health condition, smokers or ex-smokers, alcohol and drug abusers, irradiated patients, pregnancy, use of bisphosphonate therapies, blood platelet disorders, chronic sinusitis, presence of any kind of pathology in the maxillary sinus, use of medications such as immunosuppressants, and uncontrolled diabetes[16,17].

A digital panoramic radiograph was obtained for all patients before the surgical procedures, for graft augmentation and implant surgery planning. The radiographic image of each subject was used to measure and record the residual bone crest height (Table 2). For this measurement, the digital panoramic images were imported into a specific software package (UTHSCSA ImageTool software version 3.0 for Windows). Using the ruler tool in this software, the height of the remaining alveolar crest was measured. The software was calibrated using a known value to correct for image distortion that occurs during acquisition. After the sinus lift procedure, a new digital panoramic radiograph was obtained and the augmented sinus was measured as described above.

Table 1. Patient demographic data and clinical data related to the implants installed in the maxillary sinus after the augmentation procedure with the different particle sizes of Bio-Oss; N = 10 patients.

Patient	Sex	Partially or totally edentulous	Large particles		Small particles	
			Implant region	Implant length (mm)	Implant region	Implant length (mm)
1	F	Totally	16	3.75 × 10.0	26	3.75 × 8.5
1					27	3.75 × 8.5
2	F	Partially	24	3.75 × 11.5	16	3.75 × 11.5
3	M	Partially	17	3.75 × 11.5	26	3.75 × 13.0
4	F	Totally	15	3.75 × 11.5	25	3.75 × 10.0
4			16	3.75 × 13.0	26	3.75 × 10.0
5	M	Partially	16	3.75 × 10.0	26	3.75 × 11.5
6	F	Partially	24	3.75 × 13.0	14	3.75 × 11.5
6			25	3.75 × 11.5	16	3.75 × 11.5
7	F	Partially	26	3.75 × 10.0	16	3.75 × 10.0
8	M	Partially	15	3.75 × 8.5	26	3.75 × 8.5
9	F	Partially	26	3.75 × 11.5	16	3.75 × 10.0
10	M	Partially	26	3.75 × 11.5	16	3.75 × 11.5

F, female; M, male.

Table 2. Clinical data regarding the residual alveolar bone crest at the time of the surgical procedure and the increased bone height after the augmentation procedure in the maxillary sinus with both particle sizes of Bio-Oss.

Patient	Large particles			Small particles		
	Implant region	Residual bone crest height (mm)	Increased bone height postoperative (mm)	Implant region	Residual bone crest height (mm)	Increased bone height postoperative (mm)
1	16	1.25	8.75	26	2.45	6.05
1				27	3.00	5.50
2	24	2.83	8.67	16	1.07	10.43
3	17	1.35	10.15	26	2.64	10.36
4	15	2.08	9.42	25	4.01	5.99
4	16	1.78	11.22	26	4.90	5.10
5	16	1.46	8.54	26	1.50	10.00
6	24	1.95	11.05	14	1.92	9.58
6	25	1.24	10.26	16	0.88	10.62
7	26	1.59	8.41	16	1.16	8.84
8	15	1.68	6.82	26	2.13	6.37
9	26	3.48	8.02	16	3.39	6.61
10	26	4.12	7.38	16	3.85	7.65
Mean		2.07	9.21		2.53	9.06
SD		0.93	1.34		1.25	1.39
Significance[a]		NS, $P = 0.168$	NS, $P = 0.120$		NS	NS

NS, not significant; SD, standard deviation.
[a] Differences were calculated using the Wilcoxon test.

All subjects were randomly allocated to two groups by means of a random table, generated based on the radiographic images, to be grafted with either small-sized particles of DBBM (test group) or large-sized particles of DBBM (control group) (Bio-Oss; Geistlich Pharma AG).

Sinus augmentation procedure

The surgical procedures were performed as described previously, following a split-mouth design[2,6,7]. Briefly, patients received local anaesthesia with articaine 4% and adrenaline 1:100,000 (DFL, Rio de Janeiro, RJ, Brazil). A mid-crestal incision and vertical releasing incisions were made along the residual alveolar bone to access the sinus wall. A lateral window approach was performed in both the left and right sinuses to access the sinus wall, using a round diamond bur (Fig. 1), as described previously[6,7]. The surgical access respected the planned implant position and the maxillary sinus anatomy.

The sinus membrane was gently separated and gently reflected to allow the augmentation procedure. The test side was filled with small particles (0.25–1 mm) of DBBM (Bio-Oss; Geistlich Pharma AG), while the control side was filled with large-sized particles of DBBM (1–2 mm). The graft material in the sinus cavity was carefully compacted. A bioabsorbable porcine collagen barrier membrane (Bio-Gide; Geistlich Pharma AG) was used to protect the opened window to avoid epithelial tissue migration after graft placement[18], and the soft tissue was then sutured (Fig. 1).

After the maxillary sinus lifting procedure, the patients were prescribed amoxicillin 500 mg three times a day for a week, and paracetamol 750 mg every 6 hours in case of pain. Patients were instructed to wash their mouth daily with chlorhexidine mouthwash (0.2%) for 14 days starting on the day after the surgical procedure. The patients were checked regularly to verify the healing process during the first week, after which the sutures were removed. They were advised to avoid any direct contact or loading during the entire healing phase. Any sign or symptom of infection, swelling, pain, haematoma, or suppuration seen during the postoperative visits was recorded.

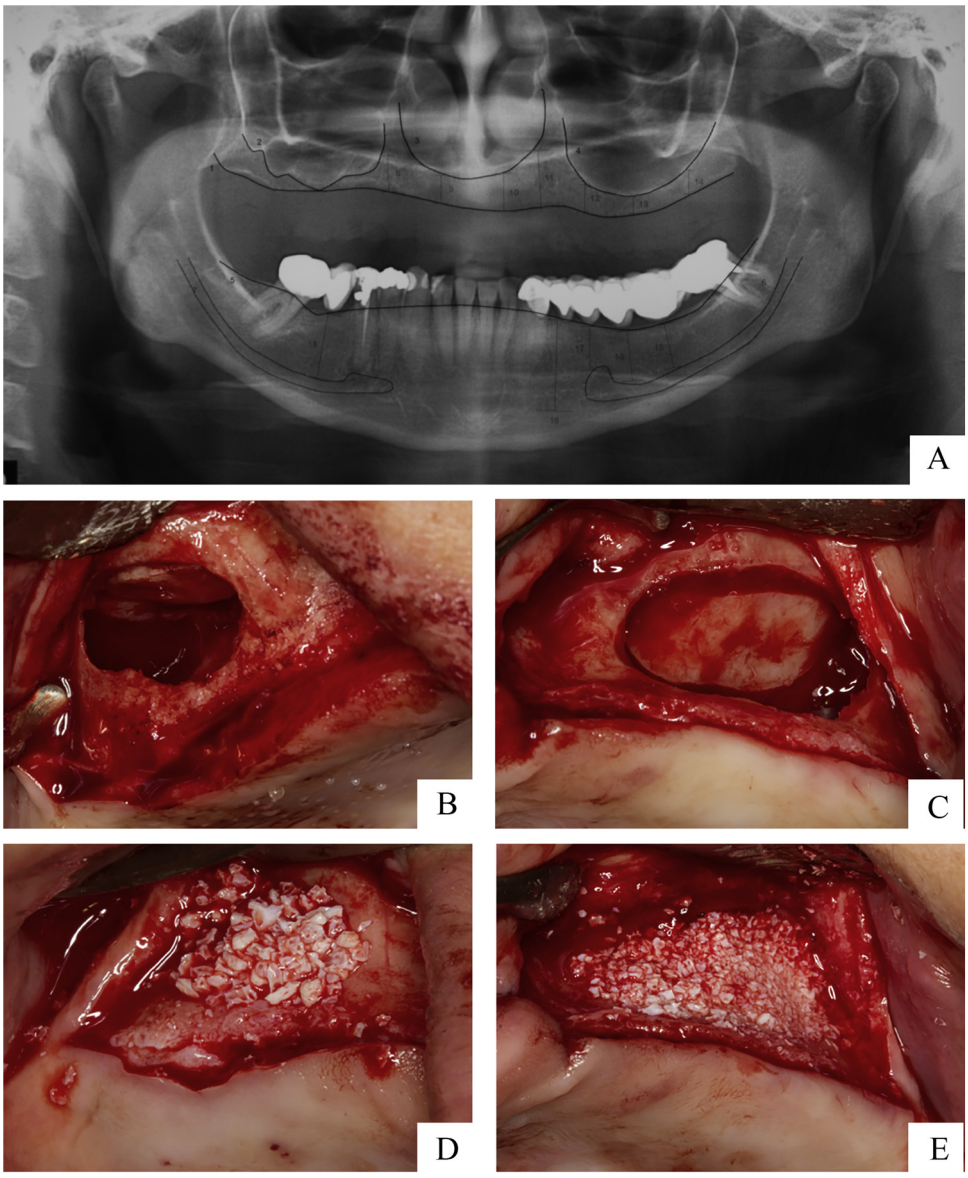

Fig. 1. Representative clinical images showing the procedure for maxillary sinus augmentation with both particle sizes of Bio-Oss. (A) Preoperative panoramic radiograph; (B) (C) photographs obtained after the lateral window approach to assess the maxillary sinuses; (D) (E) each sinus was randomly grafted with the two different particle sizes of DBBM (large particles in image D and small particles in image E).

Implant placement

After 8 months of healing, dental implants were installed in both augmented maxillary sinuses. A total of 25 double acid-etched, commercially available implants (MasterPorous; Conexao Sistemas de Protese Ltda, Arujá, São Paulo, Brazil) with an external tapered connection were inserted by the same experienced surgeon (RSF). The implants were placed according to the manufacturer's protocol, 13 on the test side and 12 on the control side. The inserted titanium implants all had a diameter of 3.75 mm; they ranged in length from 8.5 mm to 13.0 mm.

Histology and histomorphometric analysis

During implant site preparation, bone biopsies were harvested from the maxillary sinus using a trephine bur with an internal diameter of 3.0 mm and length of 15 mm (3i Implant Innovations, Florida, FL, USA). Two bone biopsy cylinders were obtained per patient (one from each sinus) in a buccal–palatal direction, i.e. perpendicular to the long axis of the implant. The biopsy included the lateral sinus wall and augmented sinus (bone graft), and the preparation depth was standardized for all samples using the markings on the trephine bur, i.e. 10 mm depth (Fig. 2).

Histological processing of the bone biopsies collected from each patient was performed according to previously published protocols[2,6,33,34]. Briefly, samples were fixed in 4% buffered formaldehyde solution for 48 hours to preserve the bone structures and subsequently decalcified in a solution of ethylenediaminetetraacetic acid (EDTA 0.5 M, pH 8) for 3 weeks at room temperature, with solution changes every 2 days. The samples were then washed for 4 hours in running water and then embedded in paraffin. Serial sections of 6 μm thickness were acquired using a semi-automatic microtome apparatus (Supercut 2065; Leica Jung,

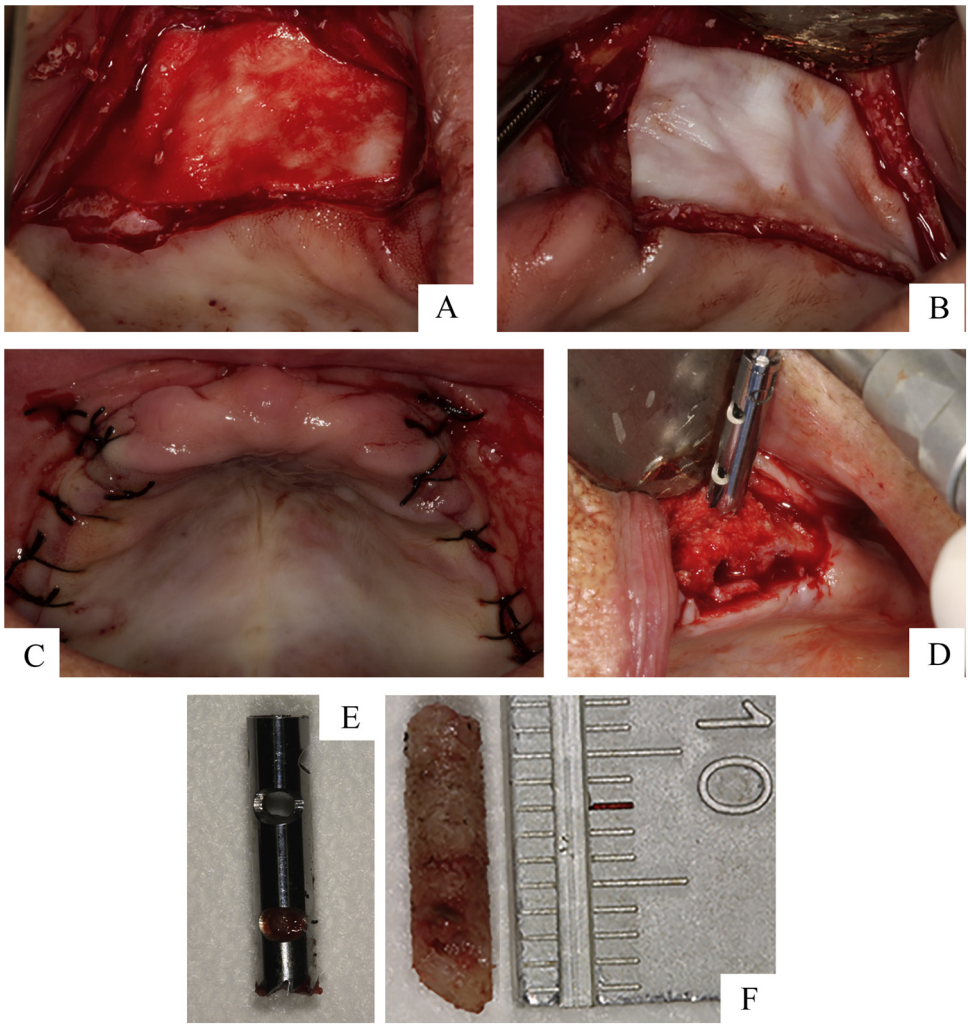

Fig. 2. (A) (B) An absorbable porcine collagen membrane was placed on both augmented sinuses to avoid epithelial tissue migration; (C) a suture was performed for primary wound closure; (D) representative image illustrating the positioning of the trephine bur to collect the bone biopsy (buccal–palatal orientation); (E) trephine bur with the collected tissue; (F) sample of the bone core.

Heidelberg, Germany). The sections were obtained along their longitudinal axis, dewaxed, rehydrated, attached to glass slides, and stained with Masson trichrome and haematoxylin and eosin (H&E). The histomorphometric measurements and descriptive histological analysis were performed using an optical microscope (Diastar; Leica, Wetzlar, Germany) connected to a high resolution digital camera interfaced to the microscope (DFC300 FX, Leica, Wetzlar, Germany).

One blinded and experienced examiner performed the descriptive and histomorphometric analyses. The digitized images were evaluated using Image J 1.45 for Windows (National Institutes of Health, USA). The descriptive histological analysis aimed to evaluate cellular characteristics, neoformed tissues, and any inflammatory reaction to the biomaterial. The histomorphometric analysis was performed to quantify the percentage of newly formed bone (bone trabeculae surrounding the graft particles with viable osteocyte cells), non-mineralized tissue, and the remnant graft particles after the healing process. Designated slides for the histological measurements followed the semi-series standard: the first section was chosen, and then four sequencing sections were excluded. Three slides per patient were used for the analysis. The bone core sample was entirely visible at the lowest magnification. The host bone site was accepted as the coronal site of the biopsies. Therefore, the region of interest (ROI) of the core sample was defined by disregarding the top and bottom areas of the biopsy (2 mm for each), with focus place on the centre of the bone where most of the graft particles were present.

A custom grid with 300 squares was constructed using Adobe Photoshop CC software (Adobe, San Jose, CA, USA) and overlapped on the digital images. The ROI for the histomorphometric measurements was represented by the whole grid that was overlaid on the centre of the bone biopsy images, and the structures below each intersection point were recorded (Fig. 3). The presence of each structure was expressed as a percentage of the total area analyzed, in accordance with previously published protocols[5,14].

Immunohistochemical analysis

The following primary antibodies were used for the IHC analysis: anti-VEGF (rabbit monoclonal anti-VEGF antibody, EP1176Y – ab52917; Abcam, Cambridge, UK); anti-OCN (mouse monoclonal anti-osteocalcin, OC4-30–ab13418; Abcam); anti-TRAP (mouse monoclonal anti-tartrate-resistant acid

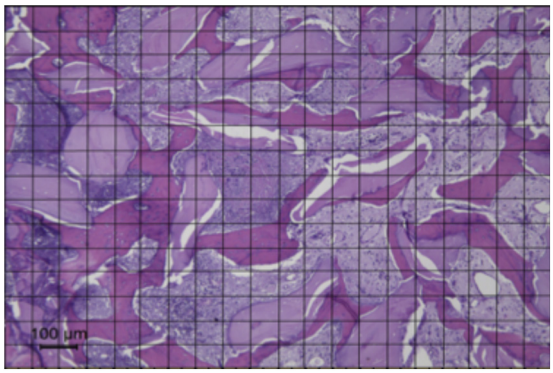

Fig. 3. Representative H&E-stained slide with the custom grid overlaid on the digital image; 300 squares were created and each of the structures at the intersection points was recorded.

phosphatase antibody, 26E5–ab49507; Abcam).

The IHC analysis was performed on 6-µm thick sections mounted on silanized slides (DAKO A/S, Glostrup, Denmark)[35,36]. Antigen retrieval was accomplished by incubation with 10 mM sodium citrate buffer (Diagnostic Biosystems, Den Haag, the Netherlands), pH 6.0 at 80 °C in a microwave, for 30 min. Antigen retrieval was performed by incubation with 0.3% hydrogen peroxide (Hydrogen Peroxidase Block; Spring Biosciences, Pleasanton, CA, USA) for 30 minutes to block endogenous peroxidase activity. Afterward, sections were incubated with Ultra V Block Protein Block (Spring Biosciences) for 30 minutes at room temperature to block non-specific protein binding. Subsequently, the slides were incubated overnight with primary antibodies, as described above. Then, a biotin-free polymer type detection method with horseradish peroxidase (HRP) conjugated with secondary antibody (Reveal Biotin-Free Polyvalent HRP; Spring Biosciences) was used, according to the manufacturer's instructions. Finally, the avidin–biotin complex (Vector Laboratories) with diaminobenzidine (DAB; Dako) as chromogen was used, and sections were counterstained with Harris haematoxylin. As a negative control, primary antibody was omitted and the sections were incubated with 1% phosphate buffered saline to assess background staining.

An experienced examiner (APSF), blinded to the two groups, evaluated the digital images (four images per sample with regular intervals of 60 µm) under an optical microscope (Leica Microsystem DM250; Leica, Wetzlar, Germany) at 200 × magnification with the aid of the LAS software (Leica Application Suite, V3). Quantification of OCN protein expression was assessed in the core central region of the biopsies using an ordinal quantitative analysis based on scores (hyper-positive +++, super-positive ++, positive +, and negative −) according to previously published studies[12,19,20]. Scores were then converted into percentile averages as follows: 0% (equivalent to '−' negative staining), 20% (equivalent to '+' 10% to 30% total staining), 60% (equivalent to '++' 50% to 70% total staining), and 90% (equivalent to '+++' 80% to 100% total staining)[12,19,20]. For VEGF and TRAP protein expression, the number of positive cells/structures was counted manually by a blinded examiner (APSF).

Statistical analysis

The data analysis was performed using GraphPad Prism software (version 8.0; GraphPad Software, Inc., La Jolla, CA, USA). All data were expressed as the mean ± standard deviation (SD). All data were submitted to the D'Agostino and Pearson test to assess the normality of the data distribution. The paired t-test and Wilcoxon test were used according to the data distribution. Differences were considered significant at $P < 0.05$.

Results

Patient characteristics

The sinus lift procedure was performed bilaterally in 10 participants (six female and four male). Following a split-mouth design, the maxillary sinuses were grafted randomly with the two different particle sizes of DBBM. Subjects ranged in age from 30 to 65 years (mean age 48.34 ± 12.83 years). Implants were placed after 8 months of healing. After the surgical intervention, none of the participants wore any provisional removable partial or total denture or fixed prosthesis. In total, 25 implants were placed in 20 maxillary sinuses. Demographic and clinical data are given in Table 1. No complications were observed during the entire healing period. The survival rate of the implants was 100%. Additionally, no complications such as migration of the graft material or opening of the wound edges were observed in the test or control group. To further minimize bias and simplify the data analysis, all implants installed were of the same width.

The residual alveolar crest height preoperative was measured on the digital panoramic images using the specific software; the findings are reported in Table 2. The preoperative crest height was 1.88 ± 0.7 mm on the side augmented with large particles and 2.53 ± 1.25 mm on the side augmented with small particles. No statistically significant difference in preoperative crest height was observed between the two particle size groups (Wilcoxon test). Eight months after the sinus augmentation procedure, the increase in ridge height was measured. The postoperative increase was 9.21 ± 1.34 mm for the side grafted with large particles and 7.93 ± 2.09 mm for the side grafted with small particles. No statistically significant difference in postoperative increase was found between the two groups.

Descriptive histological analysis

Immediately before implant placement, bone biopsies were obtained from the maxillary sinus on both sides for descriptive and histomorphometric analysis (Fig. 4). The histological appearance of the biopsies collected was very homogeneous among the patients evaluated (Fig. 4A–H). In the two experimental groups, most of the graft particles were surrounded by well-organized neoformed bone, mostly with a lamellar appearance and the presence of reversion lines. Bone trabeculae were composed of graft particles, interconnected by bridges of neoformed bone tissue.

There was a mild inflammatory reaction in both groups, and a small number of giant cells. It was possible to observe the presence of osteoclasts on the surface of the biomaterial. The spaces present between the mineralized tissues were occupied by rich vascularized connective tissue with small and large blood vessels permeating the graft particles. In this region, some areas of inflammatory infiltrate comprising mononuclear cells and fibroblasts with a fusiform morphology were observed (Fig. 4D). At increased magnification (Fig. 4G, H), it was possible to

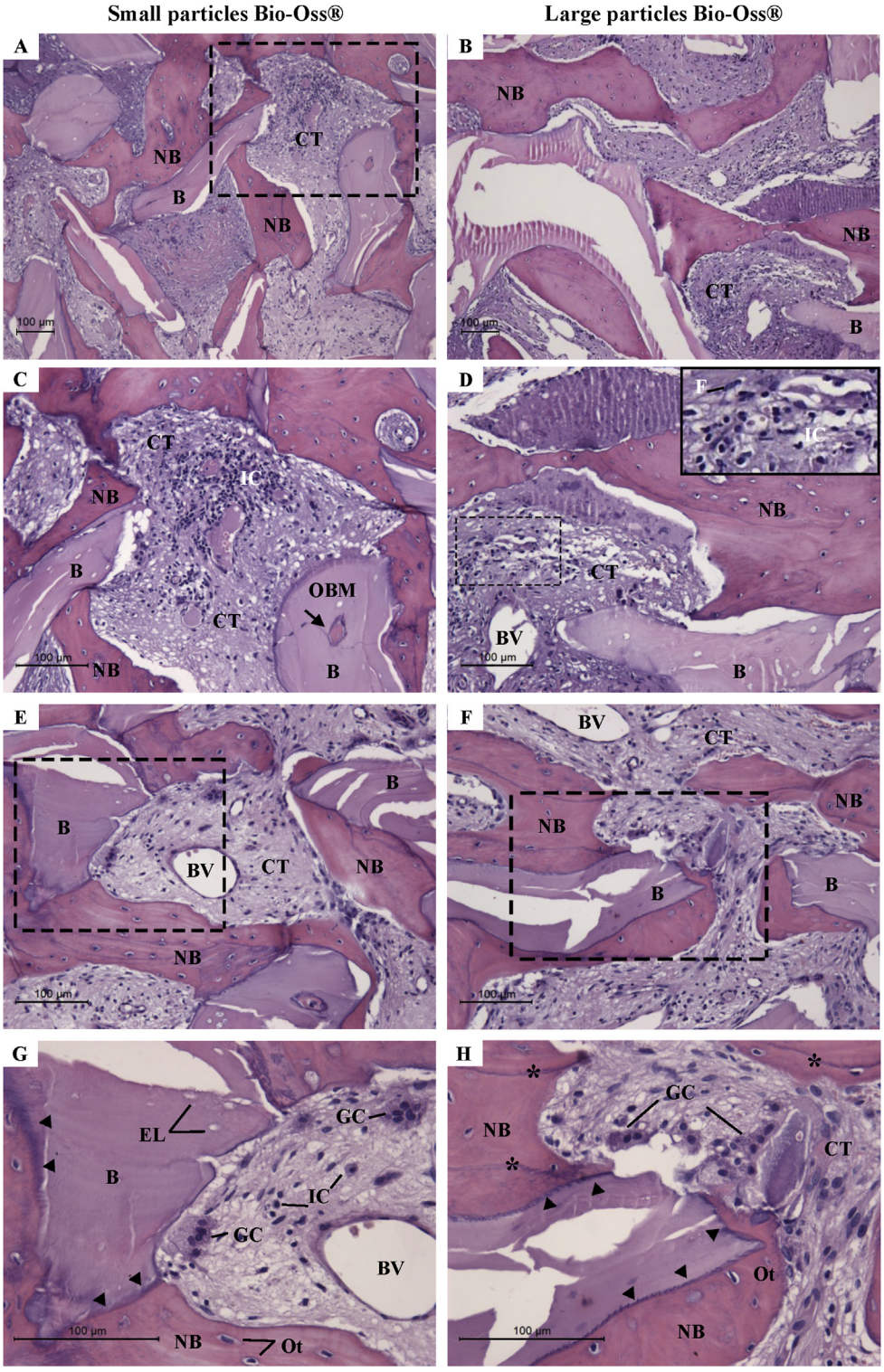

Fig. 4. Representative histological sections gathered from the maxillary sinus after 8 months of healing (H&E stain). Images A, C, E, and G are from cases in which small-sized particles of Bio-Oss were used, and images B, D, F, and H are from cases in which large-sized particles of Bio-Oss were used. NB, newly formed bone; B, biomaterial; CT, connective tissue; OBM, organic bone marrow; F, fibroblast; IC, inflammatory cells; BV, blood vessel; EL, empty lacunae; GC, giant cell; Ot, osteocyte. Asterisks (*) indicate the reversal lines; arrowheads indicate the interface between biomaterial and new bone with basophilic aspect. Inset in image D is a magnification of the smaller rectangular area (dotted lines). Rectangular areas in images E and F correspond to the magnified areas in images G and H, respectively. Bars represent 100 µm.

observe that both particle sizes were in close contact with the neoformed bone and with a pronounced basophilic interface. The newly formed bone presented numerous osteocytes in wide gaps. Several osteoblasts were observed on the surface of the neoformed bone, which were polarized and intensely basophilic. In both groups, it was observed that the three-dimensional aspect of the particles had allowed invasion by the neoformed bone tissue and blood vessels into the biomaterial pores. The presence of osteoblasts and osteocytes inside the bone lacunae can be seen in Fig. 5A–D. Moreover, reversal lines surrounding the bone tissue are evident.

Masson trichrome staining (Fig. 5E, F) revealed that for both types of graft material there was intimate contact between the neoformed bone and biomaterial (arrowheads). The interface between bone tissue and graft material was seen to be mainly basophilic (arrowheads). The reversal line was observed in the bone tissue. The neoformed bone exhibited numerous osteocytes in large lacunae. Empty lacunae were observed inside the organic structure. Giant cells were also noted.

Histomorphometric analysis

Histomorphometric analysis did not reveal any statistically significant difference in the percentage of remaining biomaterial ($32.4 \pm 8.56\%$ and $38.0 \pm 6.92\%$), newly formed bone ($36.1 \pm 9.60\%$ and $36.7 \pm 5.79\%$), or connective/fibrous tissue ($30.4 \pm 8.63\%$ and $23.8 \pm 6.16\%$) between the groups treated with small- and large-sized particles of Bio-Oss, respectively (Fig. 5G).

Immunohistochemical analysis

IHC analysis of protein expression of VEGF, OCN, and TRAP was performed on histological slides. After VEGF staining, the number of blood vessels did not differ significantly between the small-sized particle group and the large-sized particle group (Fig. 6). Accordingly, the number of TRAP-positive cells did not differ between the two groups (Fig. 7). Furthermore, protein expression of OCN was similar for the two sizes of Bio-Oss (Fig. 8).

Discussion

The maxillary sinus augmentation procedure is indicated in cases with severe bone crest resorption, to provide structural and mechanical support for the installation of appropriate length implants in the posterior area of the maxilla[7–9,14]. Several biomaterials have been proposed in the literature to fill the maxillary sinus and have presented successful clinical outcomes for bone regeneration[21–24]. Bio-Oss is one of these materials and is among the most utilized graft materials for sinus augmentation due to its characteristics similar to those of human cancellous bone, including crystallinity and physical and morphological properties. DBBM acts as a scaffold and matrix for osteogenic cell migration from the sinus wall to the graft, increasing the capability of new bone formation[3,4]. Although several studies evaluating bone healing after sinus floor augmentation with DBBM have been conducted, available data on the expression of proteins involved in bone metabolism after sinus augmentation using different particle sizes of Bio-Oss appear to be limited. The aim of this study was to investigate the clinical effects of small- and large-sized particles of DBBM at 8 months after maxillary sinus augmentation by means of descriptive, histomorphometric, and IHC analyses. The study findings demonstrated that both particle sizes of Bio-Oss performed equally well, with a high implant survival rate and no difference in any of the parameters evaluated. This study appears to be unique in evaluating different particle sizes of DBBM using IHC analysis.

Descriptive and histomorphometric evaluation demonstrated that both particle sizes were surrounded by well-organized neoformed bone ($36.1 \pm 9.60\%$ and $36.7 \pm 5.79\%$), mostly with a lamellar appearance and the presence of reversion lines and connective/fibrous tissue ($30.4 \pm 8.63\%$ and $23.8 \pm 6.16\%$) (small-size and large-size particles of Bio-Oss, respectively) (Fig. 2A–G). The percentage of remaining biomaterial ($32.4 \pm 8.56\%$ and $38.0 \pm 6.92\%$) was also similar for the two particle sizes. The spaces present between the mineralized tissues were occupied by a rich vascularized connective tissue with small and large blood vessels in close proximity to the graft particles. Furthermore, giant cells, probably osteoclasts, were observed in contact with the biomaterial. Both particle sizes presented the same amount of osteoclast-like cells and slight inflammatory infiltrate. The histological data are in agreement with those of a previous report that showed similar features after sinus lifting with these two DBBM preparations[8]. However, Testori et al.[9] recently showed histomorphometrically that large particles of Bio-Oss resulted in a higher amount of newly formed bone compared to small particles ($26.77 \pm 9.63\%$ and $18.77 \pm 4.74\%$, respectively). These contradictory findings might be accounted for by differences in patient characteristics, sinus anatomy, surgical technique, and/or sample size.

Bio-Oss is characterized by a relatively low resorption rate after placement in the maxillary sinus because it lacks osteogenic properties. For this reason the maturation of this type of material may take up to 8 months, which is considerably longer than for autogenous bone[25]. This means that several graft particles will not be fully resorbed before implant placement. Therefore, there will be reduced space between the graft particles for bone neoformation, which might explain the outcomes of the present study in regard to the amount of new bone formation and the remaining biomaterial in the two groups.

IHC analyses showed significant evidence concerning cell behaviour centred on the expression of proteins involved in bone metabolism after 8 months of healing before implant placement. OCN is expressed by osteoblasts and binds to hydroxyapatite of bone matrix[12]. OCN play an important role in bone maturation and is only found after the end of osteoblast proliferation activity, representative of the differentiated and mature stage of those cells[26]. The study results demonstrated that both particle sizes presented the same positive immunolabelling for protein expression of OCN. TRAP is a protein related to bone resorption and plays a pivotal role as a marker of osteoclastic activity. The study data showed that TRAP-positive cells were positively stained, without any difference between the two preparations. This means that the graft biomaterial, independent of the particle size, presented considerable osteoclastic activity aimed at resorbing the DBBM graft material and gradually replacing it with newly formed bone.

Protein expression of VEGF, a strong and key modulator of vascular formation, was also evaluated in the histological sections. VEGF supports angiogenesis by triggering endothelial cells[27–29]. A cumulative body of evidence has demonstrated that VEGF presents several other functions, such as improvement in bone formation by transporting mesenchymal cells to the mineralized area by means of newly formed vessels, and osteoblast and osteoclast differentiation. According to a previous study[30], endothelial cells are frequently found in areas where new bone is produced. IHC analysis of VEGF did not show any statistically significant

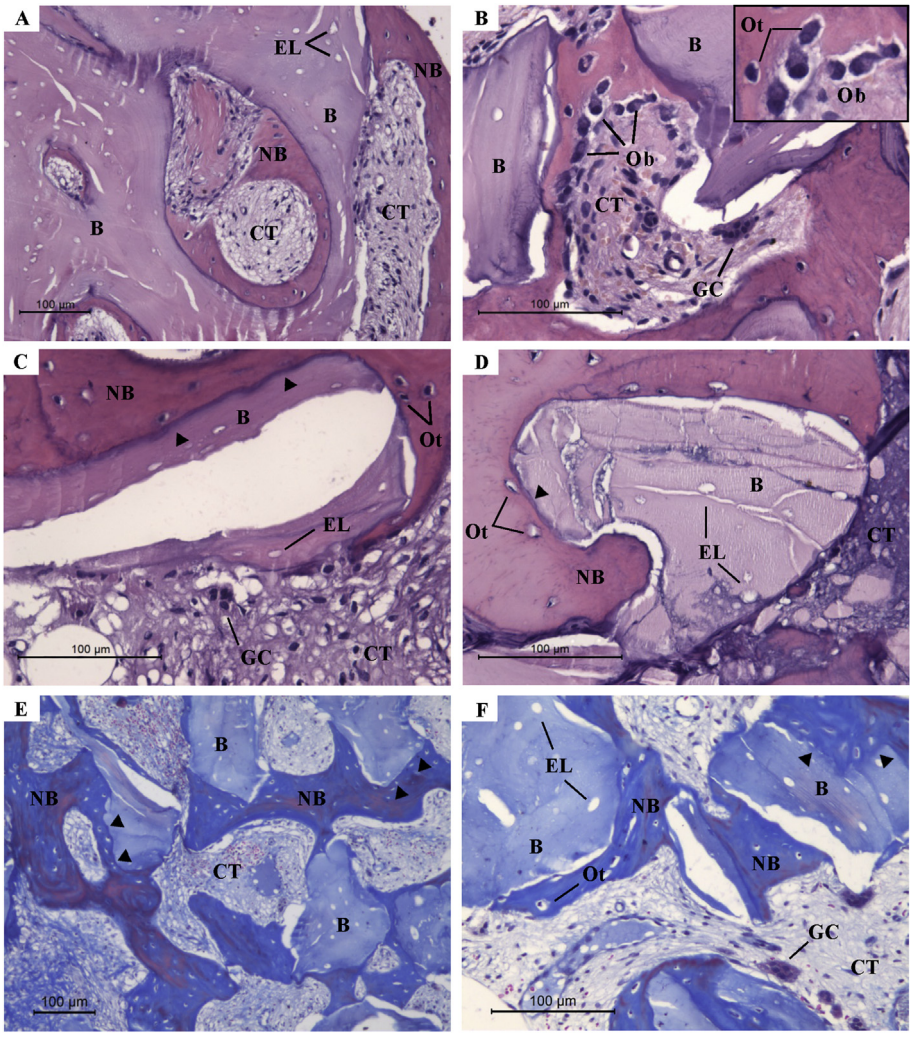

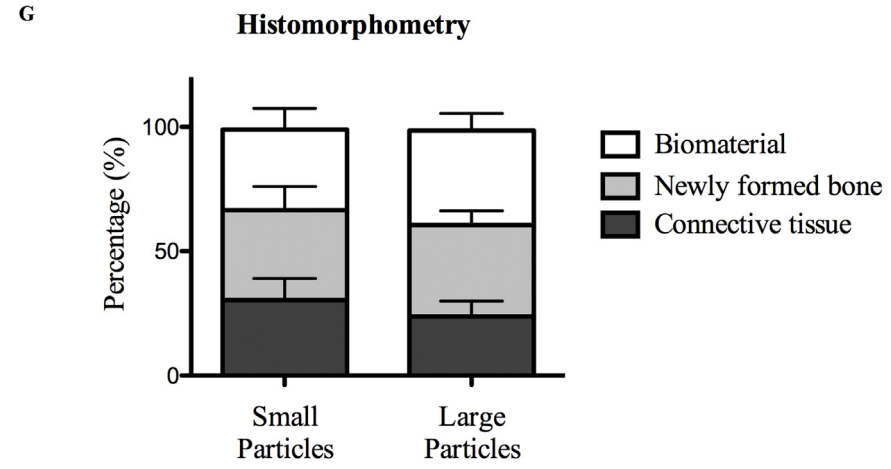

Fig. 5. Representative histological sections from cases in which small-sized particles of Bio-Oss were used (A–E) and cases in which large-sized particles of Bio-Oss were used (F), stained with H&E (A–D) and Masson trichrome (E, F). NB, newly formed bone; B, biomaterial; CT, connective tissue; EL, empty lacunae; GC, giant cell; Ot, osteocyte. Arrowheads indicate the interface between biomaterial and new bone with basophilic aspect. Inset in image B is a magnification of part of the same image. Image G shows the quantification of histomorphometric findings: percentage of newly formed bone, biomaterial, and connective tissue. Differences between the groups were calculated by paired t-test or Wilcoxon text. Data represent the mean ± standard deviation.

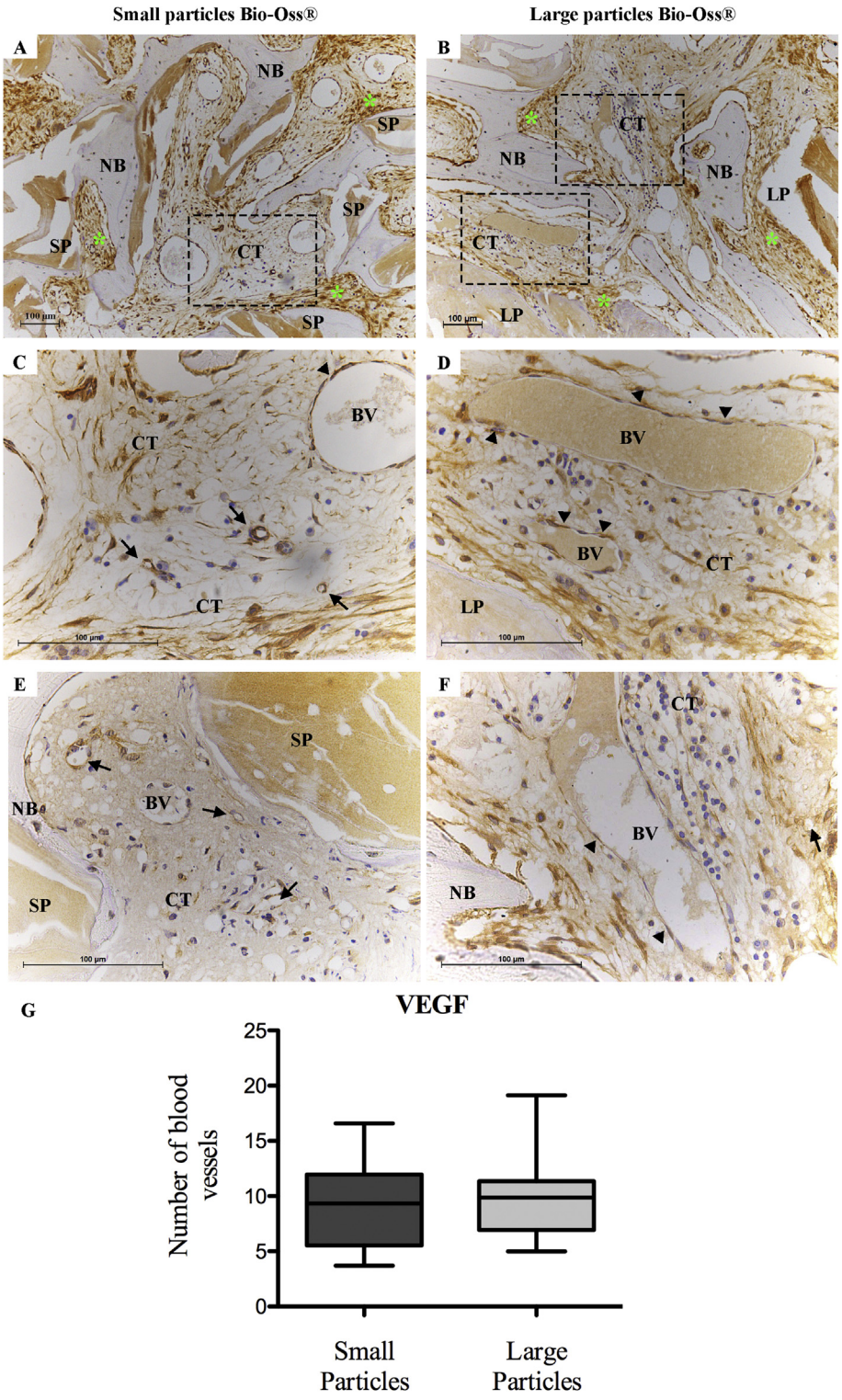

Fig. 6. Representative immunohistochemical sections for VEGF in cases in which small-sized particles of Bio-Oss were used (A, C, E) and cases in which large-sized particles of Bio-Oss were used (B, D, F). NB, newly formed bone; SP, small particles of graft; LP, large particles of graft; CT, connective tissue; BV, blood vessel. Green asterisks (*) indicate VEGF-positive staining; arrowheads indicate large blood vessels stained positively for VEGF; arrows indicate small blood vessels stained positively for VEGF. The small outlined rectangles in images A and B correspond to magnified areas in images C–F. Image G shows the quantification of the numbers of blood vessels positively stained for VEGF in the two groups. Differences between the groups were calculated by paired t-test or Wilcoxon text. Data represent the mean ± standard deviation.

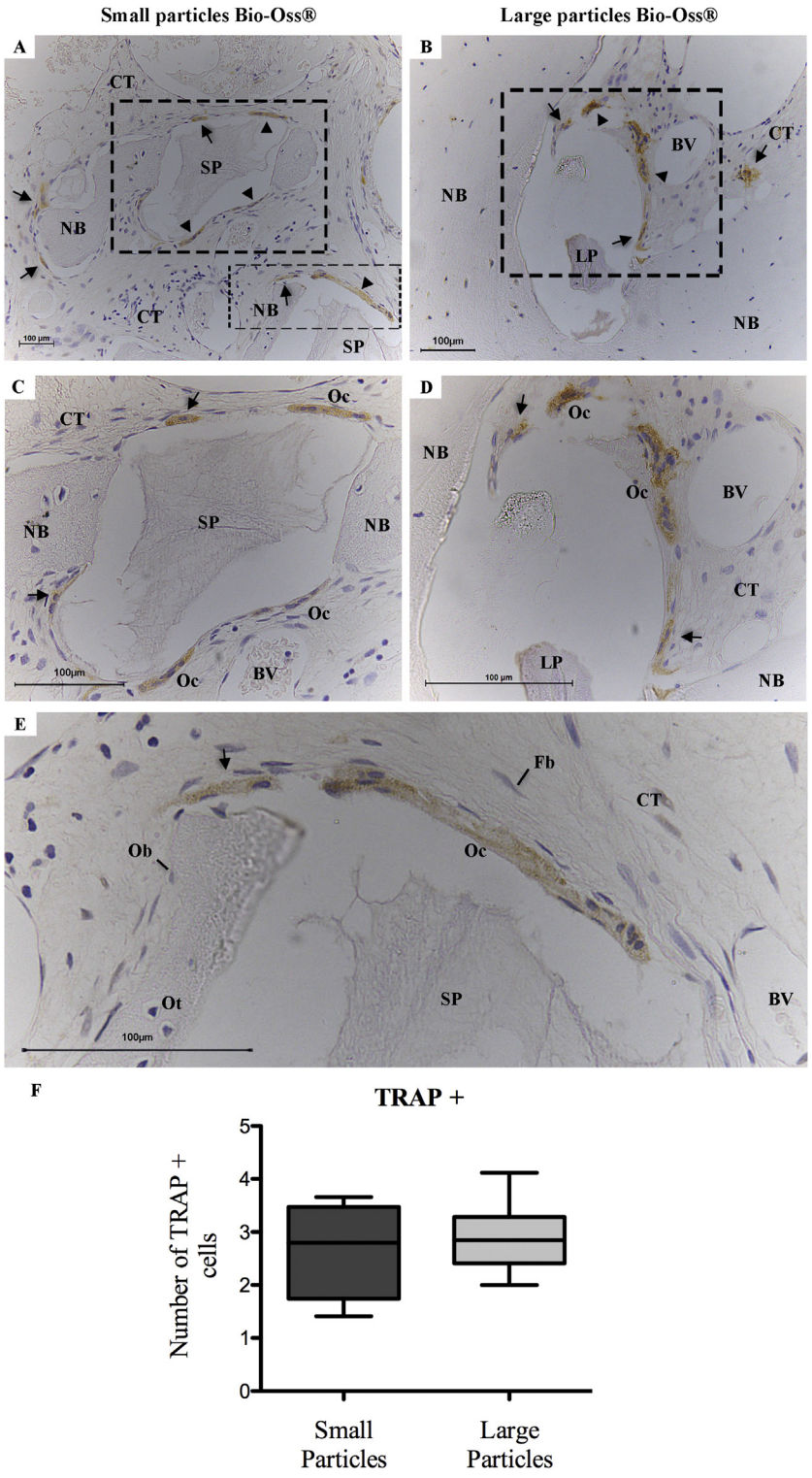

Fig. 7. Representative immunohistochemical sections for TRAP in cases in which small-sized particles of Bio-Oss were used (A, C, E) and cases in which large-sized particles of Bio-Oss were used (B, D). NB, newly formed bone; SP, small particles of graft; LP, large particles of graft; CT, connective tissue; Fb, fibroblast; Oc, osteoclast; Ob, osteoblast; Ot, osteocyte; BV, blood vessel. Arrows indicate positive immunolabelling for TRAP around the biomaterial; arrowheads indicate stained osteoclasts. The dotted rectangular areas in images A and B correspond to magnified areas in images C, D, and E. Image F shows the quantification of immunolabelling for TRAP-positive cells in the two groups. Differences between the groups were calculated by paired t-test or Wilcoxon text. Data represent the mean ± standard deviation.

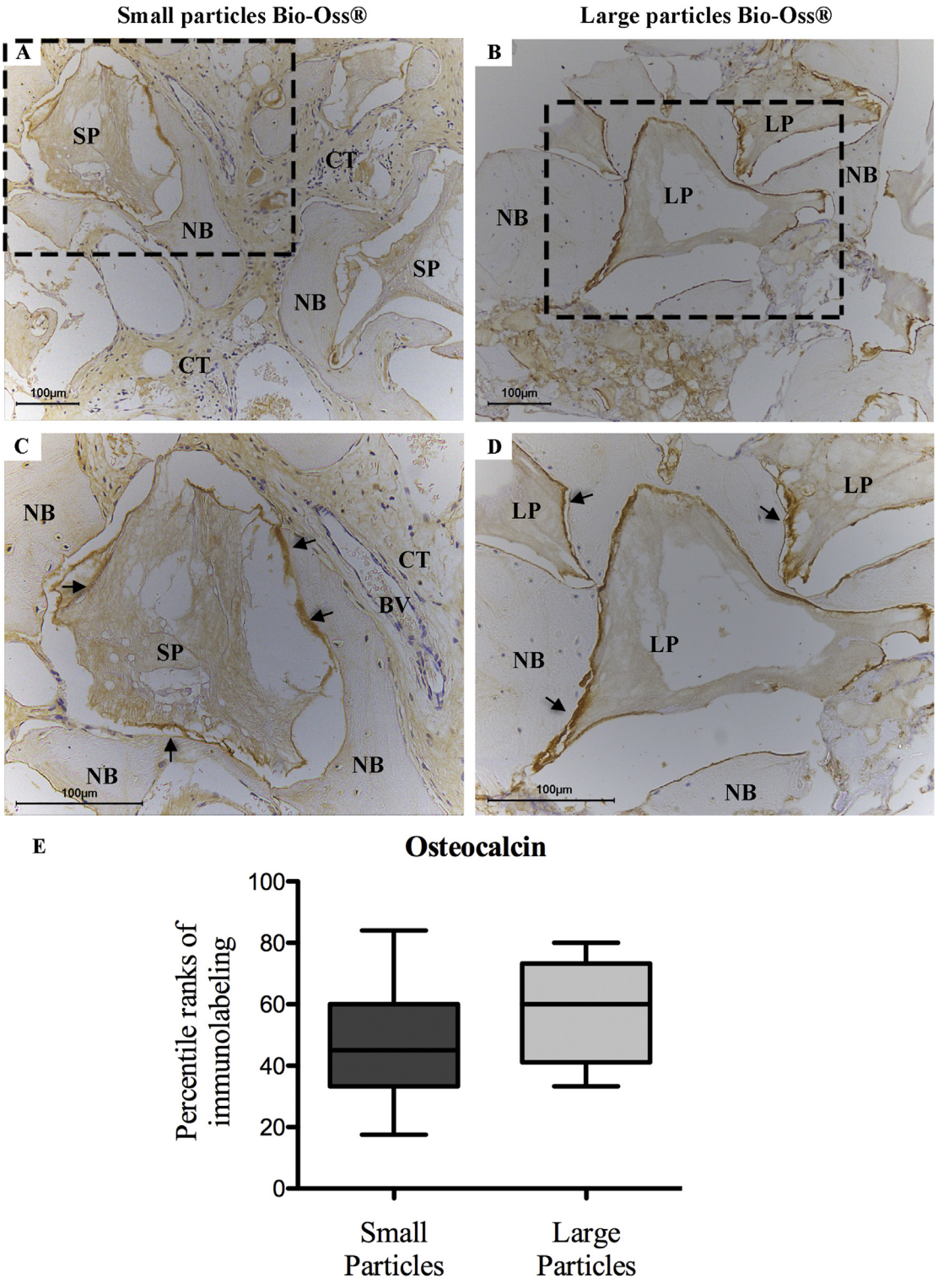

Fig. 8. Representative immunohistochemical sections for OCN in cases in which small-sized particles of Bio-Oss were used (A, C) and cases in which large-sized particles of Bio-Oss were used (B, D). NB, newly formed bone; SP, small particles of graft; LP, large particles of graft; CT, connective tissue. Arrows indicate positive immunolabelling for OCN around the biomaterial. The dotted rectangular areas in images A and B correspond to magnified areas in images C and D. Image E shows the quantification of immunolabelling for OCN in the two groups. Differences between the groups were calculated by paired t-test or Wilcoxon text. Data represent the mean ± standard deviation.

difference between the two groups, and this fact could be attributed to the long period of healing (8 months) up until the time of bone harvesting. According to a previous study, after 60 days of healing, VEGF expression tends to decrease over time compared to the initial period of healing[31].

An interesting fact that should be mentioned is the smaller amount of graft material needed when large particles of Bio−Oss are used to complete a sinus floor augmentation procedure when compared to the small particle size. From a practical standpoint, with large−sized particles the quantity of bone biomaterial used to fill the sinus cavity can be safely reduced without compromising the final graft volume. Additionally, the choice of small− or large−sized particles is dependent on surgeon preference, the size of the maxillary sinus, number of implants necessary for rehabilitation, and sinus anatomy. The findings of this study are in parallel with observations made in our previous study, in which no difference was found between the two particle sizes in relation to the implant insertion torque or implant stability[7].

An interesting aspect that was not addressed in the study was whether an early intervention for biopsy harvesting would have shown more precise features of the healing dynamics. It is expected that changes in the healing process occur soon after graft placement before remodelling of the biomaterial particles. However, previous studies have shown that a healing period of at least 6 months should be allowed for safe placement of the dental implants in a maxillary sinus grafted with DBBM[8,32]. In this regard, the healing period was extended to 8 months to allow maturation of the graft. Another consideration that should be mentioned is that the residual alveolar crest height preoperative and the augmented sinuses (postoperative) were measured by means of digital panoramic radiographs. Two-dimensional radiography often results in distortion of the images. To minimize this bias, specific and calibrated software was used (UTHSCSA Image Tool software) with a known value to accurately measure the remaining alveolar crest. Cone beam computed tomography would have provided more precise measurements and should be recommended to evaluate bone dimensions both pre- and post-surgical intervention. Finally, the sinus anatomy and sinus volume were not measured in this study. This would provide useful complementary information about the biomaterial and bone healing and remodelling. For all of these reasons, further randomized controlled clinical trials are warranted before definitive conclusions can be drawn about the dynamics of the healing process.

In summary, using descriptive, histomorphometric, and IHC analyses to evaluate the effects of different preparations of Bio-Oss, it was demonstrated that there was no difference in any of the parameters evaluated, including newly formed bone, amount of remaining biomaterial, or connective tissue in the maxillary sinus. Furthermore, protein expression of OCN, VEGF, and TRAP did not differ between the two groups. Indeed, both particle sizes were effective for bone neoformation, performed equally well, and presented optimal properties, therefore supporting their possible use as graft material for implant placement after maxillary sinus floor augmentation.

Acknowledgements. We are extremely grateful to Geistlich Pharma AG for the free donation of the small and large particles of Bio-Oss used in this study. FUNADESP – Fundacao Nacional de Desenvolvimento do Ensino Superior Particular.

Funding. None.

Competing interests. None.

Ethical approval. Approval for this study was obtained from the Ethics Committee on Human Research before patient enrolment (protocol #580.869). In addition, written informed consent was obtained from each subject who participated in the study.

Patient consent. Subjects were fully informed about the treatment and implications, and written informed consent was obtained prior to the commencement of treatment.

References

1. Boyne PJ, James RA. Grafting of the maxillary sinus floor with autogenous marrow and bone. *J Oral Surg* 1980;**38**:613–6.
2. Pichotano EC, de Molon RS, Freitas de Paula LG, de Souza RV, Marcantonio Jr E, Zandim-Barcelos DL. Early placement of dental implants in maxillary sinus grafted with leukocyte and platelet-rich fibrin (L-PRF) and deproteinized bovine bone mineral. *J Oral Implantol* 2018;**44**:199–206.
3. Browaeys H, Bouvry P, De Bruyn H. A literature review on biomaterials in sinus augmentation procedures. *Clin Implant Dent Relat Res* 2007;**9**:166–77.
4. Tadjoedin ES, de Lange GL, Bronckers AL, Lyaruu DM, Burger EH. Deproteinized cancellous bovine bone (Bio-Oss) as bone substitute for sinus floor elevation. A retrospective, histomorphometrical study of five cases. *J Clin Periodontol* 2003;**30**:261–70.
5. Valentini P, Abensur DJ. Maxillary sinus grafting with anorganic bovine bone: a clinical report of long-term results. *Int J Oral Maxillofac Implants* 2003;**18**:556–60.
6. de Molon RS, de Paula WN, Spin-Neto R, Verzola MH, Tosoni GM, Lia RC, Scaf G, Marcantonio Jr E. Correlation of fractal dimension with histomorphometry in maxillary sinus lifting using autogenous bone graft. *Braz Dent J* 2015;**26**:11–8.
7. Dos Anjos TL, de Molon RS, Paim PR, Marcantonio E, Marcantonio Jr E, Faeda RS. Implant stability after sinus floor augmentation with deproteinized bovine bone mineral particles of different sizes: a prospective, randomized and controlled split-mouth clinical trial. *Int J Oral Maxillofac Surg* 2016;**45**:1556–63.
8. Chackartchi T, Iezzi G, Goldstein M, Klinger A, Soskolne A, Piattelli A, Shapira L. Sinus floor augmentation using large (1–2 mm) or small (0.25–1 mm) bovine bone mineral particles: a prospective, intra-individual controlled clinical, micro-computerized tomography and histomorphometric study. *Clin Oral Implants Res* 2011;**22**:473–80.
9. Testori T, Wallace SS, Trisi P, Capelli M, Zuffetti F, Del Fabbro M. Effect of xenograft (ABBM) particle size on vital bone formation following maxillary sinus augmentation: a multicenter, randomized, controlled, clinical histomorphometric trial. *Int J Periodontics Restorative Dent* 2013;**33**:467–75.
10. Galindo-Moreno P, Hernandez-Cortes P, Aneiros-Fernandez J, Camara M, Mesa F, Wallace S, O'Valle F. Morphological evidences of Bio-Oss colonization by CD44-positive cells. *Clin Oral Implants Res* 2014;**25**:366–71.
11. Kazemi E, Dadfarnia S, Haji Shabani AM, Ranjbar M. Synthesis, characterization, and application of a Zn (II)-imprinted polymer grafted on graphene oxide/magnetic chitosan nanocomposite for selective extraction of zinc ions from different food samples. *Food Chem* 2017;**237**:921–8.
12. Dos Santos PL, de Molon RS, Queiroz TP, Okamoto R, de Souza Faloni AP, Gulinelli JL, Luvizuto ER, Garcia Jr IR. Evaluation of bone substitutes for treatment of peri-implant bone defects: biomechanical, histological, and immunohistochemical analyses in the rabbit tibia. *J Periodontal Implant Sci* 2016;**46**:176–96.

13. de Molon RS, de Avila ED, Cirelli JA, Mollo Fde Jr A, de Andrade MF, Filho LA, Barros LA. A combined approach for the treatment of resorbed fresh sockets allowing immediate implant restoration: a 2-year follow-up. *J Oral Implantol* 2015;**41**:712–8.
14. Mordenfeld A, Hallman M, Johansson CB, Albrektsson T. Histological and histomorphometrical analyses of biopsies harvested 11 years after maxillary sinus floor augmentation with deproteinized bovine and autogenous bone. *Clin Oral Implants Res* 2010;**21**:961–70.
15. Schulz KF, Altman DG, Moher D, CONSORT Group. CONSORT Statement: updated guidelines for reporting parallel group randomised trials. *BMC Med* 2010;**8**:18.
16. de Molon RS, Sakakura CE, Faeda RS, Sartori R, Palhares D, Margonar R, Marcantonio Jr E. Effect of the long-term administration of cyclosporine A on bone healing around osseointegrated titanium implants: a histomorphometric study in the rabbit tibia. *Microsc Res Tech* 2017;**80**:1000–8.
17. de Molon RS, Morais-Camilo JA, Verzola MH, Faeda RS, Pepato MT, Marcantonio Jr E. Impact of diabetes mellitus and metabolic control on bone healing around osseointegrated implants: removal torque and histomorphometric analysis in rats. *Clin Oral Implants Res* 2013;**24**:831–7.
18. Wallace SS, Froum SJ. Effect of maxillary sinus augmentation on the survival of endosseous dental implants. A systematic review. *Ann Periodontol* 2003;**8**:328–43.
19. Esteves JC, Marcantonio Jr E, de Souza Faloni AP, Rocha FR, Marcantonio RA, Wilk K, Intini G. Dynamics of bone healing after osteotomy with Piezosurgery or conventional drilling—histomorphometrical, immunohistochemical, and molecular analysis. *J Transl Med* 2013;**11**:221.
20. Kim YJ, de Molon RR, Horiguti FR, Contador GP, Coelho MA, Mascarenhas VI, de Souza Faloni AP, Cirelli JA, Sendyk WR. Vertical bone augmentation using deproteinized bovine bone mineral, absorbable collagen sponge, and recombinant human bone morphogenetic protein-2: an in vivo study in rabbits. *Int J Oral Maxillofac Implants* 2018;**33**:512–22.
21. Alayan J, Ivanovski S. A prospective controlled trial comparing xenograft/autogenous bone and collagen-stabilized xenograft for maxillary sinus augmentation—complications, patient-reported outcomes and volumetric analysis. *Clin Oral Implants Res* 2018;**29**:248–62.
22. Comert Kilic S, Gungormus M, Parlak SN. Histologic and histomorphometric assessment of sinus-floor augmentation with beta-tricalcium phosphate alone or in combination with pure-platelet-rich plasma or platelet-rich fibrin: a randomized clinical trial. *Clin Implant Dent Relat Res* 2017;**19**:959–67.
23. Helder MN, van Esterik FA, Kwehandjaja MD, Ten Bruggenkate CM, Klein-Nulend J, Schulten E. Evaluation of a new biphasic calcium phosphate for maxillary sinus floor elevation: micro-CT and histomorphometrical analyses. *Clin Oral Implants Res* 2018;**29**:488–98.
24. Kolerman R, Nissan J, Rahmanov M, Vered H, Cohen O, Tal H. Comparison between mineralized cancellous bone allograft and an alloplast material for sinus augmentation: a split mouth histomorphometric study. *Clin Implant Dent Relat Res* 2017;**19**:812–20.
25. Choukroun J, Diss A, Simonpieri A, Girard MO, Schoeffler C, Dohan SL, Dohan AJ, Mouhyi J, Dohan DM. Platelet-rich fibrin (PRF): a second-generation platelet concentrate. Part V: histologic evaluations of PRF effects on bone allograft maturation in sinus lift. *Oral Surg Oral Med Oral Pathol Oral Radiol Endod* 2006;**101**:299–303.
26. Thorwarth M, Rupprecht S, Falk S, Felszeghy E, Wiltfang J, Schlegel KA. Expression of bone matrix proteins during de novo bone formation using a bovine collagen and platelet-rich plasma (PRP)—an immunohistochemical analysis. *Biomaterials* 2005;**26**:2575–84.
27. Kim JE, Kang SS, Choi KH, Shim JS, Jeong CM, Shin SW, Huh JB. The effect of anodized implants coated with combined rhBMP-2 and recombinant human vascular endothelial growth factors on vertical bone regeneration in the marginal portion of the peri-implant. *Oral Surg Oral Med Oral Pathol Oral Radiol* 2013;**115**:e24–31.
28. Ferrara N, Gerber HP, LeCouter J. The biology of VEGF and its receptors. *Nat Med* 2003;**9**:669–76.
29. Senger DR, Van de Water L, Brown LF, Nagy JA, Yeo KT, Yeo TK, Berse B, Jackman RW, Dvorak AM, Dvorak HF. Vascular permeability factor (VPF, VEGF) in tumor biology. *Cancer Metastasis Rev* 1993;**12**:303–24.
30. Deckers MM, Karperien M, van der Bent C, Yamashita T, Papapoulos SE, Lowik CW. Expression of vascular endothelial growth factors and their receptors during osteoblast differentiation. *Endocrinology* 2000;**141**:1667–74.
31. Faria PE, Okamoto R, Bonilha-Neto RM, Xavier SP, Santos AC, Salata LA. Immunohistochemical, tomographic and histological study on onlay iliac grafts remodeling. *Clin Oral Implants Res* 2008;**19**:393–401.
32. Nizam N, Eren G, Akcali A, Donos N. Maxillary sinus augmentation with leukocyte and platelet-rich fibrin and deproteinized bovine bone mineral: a split-mouth histological and histomorphometric study. *Clin Oral Implants Res* 2018;**29**:67–75.
33. Faloni AP, Sasso-Cerri E, Rocha FR, Katchburian E, Cerri PS. Structural and functional changes in the alveolar bone osteoclasts of estrogen-treated rats. *J Anat* 2012;**220**:77–85. http://dx.doi.org/10.1111/j.1469-7580.2011.01449.x. Epub 2011 Nov 16.
34. Faloni AP, Sasso-Cerri E, Katchburian E, Cerri PS. Decrease in the number and apoptosis of alveolar bone osteoclasts in estrogen-treated rats. *J Periodontal Res* 2007;**42**:193–201.
35. Esteves JC, Marcantonio Jr E, de Souza Faloni AP, Rocha FR, Marcantonio RA, Wilk K, Intini G. Dynamics of bone healing after osteotomy with piezosurgery or conventional drilling – histomorphometrical, immunohistochemical, and molecular analysis. *J Transl Med* 2013;**11**:221. http://dx.doi.org/10.1186/1479-5876-11-221.
36. Esteves JC, de Souza Faloni AP, Macedo PD, Nakata PB, Chierici Marcantonio RA, Intini G, Marcantonio Jr E. Effects on bone repair of osteotomy with drills or with erbium, chromium: yttrium-scandium-gallium-garnet laser: histomorphometric and immunohistochemical study. *J Periodontol* 2016;**87**:452–60. http://dx.doi.org/10.1902/jop.2015.150406. Epub 2015 Dec 22.

Address:
Rafael Scaf de Molon
Department of Diagnosis and Surgery
School of Dentistry at Araraquara – São Paulo State University
1680 Humaita Street
14801-903 Araraquara
São Paulo
Brazil
Tel: +55 16 997309293. Fax: +55 16 33016300
rafaelsmolon@gmail.com,
molon.foar@yahoo.com.br,
rafael.molon@unesp.br